RBM24 promotes U1 snRNP recognition of the mutated 5′ splice site in the *IKBKAP* gene of familial dysautonomia

KENJI OHE,[1,2,8] MAYUMI YOSHIDA,[1,9] AKIKO NAKANO-KOBAYASHI,[1] MOTOYASU HOSOKAWA,[1] YUKIYA SAKO,[1] MAKI SAKUMA,[1] YUKIKO OKUNO,[3] TOMOMI USUI,[4] KENSUKE NINOMIYA,[1,10] TAKAYUKI NOJIMA,[5] NAOYUKI KATAOKA,[6,7] and MASATOSHI HAGIWARA[1]

[1]Department of Anatomy and Developmental Biology, Kyoto University Graduate School of Medicine, Sakyo-ku, Kyoto 606-8501, Japan
[2]Training Program of Leaders for Integrated Medical System for Fruitful Healthy-Longevity Society (LIMS), Kyoto University Graduate School of Medicine, Sakyo-ku, Kyoto 606-8501, Japan
[3]Medical Research Support Center, Kyoto University Graduate School of Medicine, Sakyo-ku, Kyoto 606-8501, Japan
[4]Laboratory of Gene Expression, School of Biomedical Science, Tokyo Medical and Dental University, Bunkyo-ku, Tokyo 113-8510, Japan
[5]Sir William Dunn School of Pathology, University of Oxford, Oxford OX1 3RE, United Kingdom
[6]Laboratory for Malignancy Control Research, Medical Innovation Center, Kyoto University Graduate School of Medicine, Sakyo-ku, Kyoto 606-8507, Japan
[7]Laboratory of Cell Regulation, Departments of Applied Animal Sciences and Applied Biological Chemistry, Graduate School of Agriculture and Life Sciences, The University of Tokyo, Bunkyo-ku, Tokyo 113-8657, Japan

ABSTRACT

The 5′ splice site mutation (IVS20+6T>C) of the *inhibitor of κ light polypeptide gene enhancer in B cells, kinase complex-associated protein* (*IKBKAP*) gene in familial dysautonomia (FD) is at the sixth intronic nucleotide of the 5′ splice site. It is known to weaken U1 snRNP recognition and result in an aberrantly spliced mRNA product in neuronal tissue, but normally spliced mRNA in other tissues. Aberrantly spliced *IKBKAP* mRNA abrogates IKK complex-associated protein (IKAP)/elongator protein 1 (ELP1) expression and results in a defect of neuronal cell development in FD. To elucidate the tissue-dependent regulatory mechanism, we screened an expression library of major RNA-binding proteins (RBPs) with our mammalian dual-color splicing reporter system and identified RBM24 as a regulator. RBM24 functioned as a cryptic intronic splicing enhancer binding to an element (IVS20+13–29) downstream from the intronic 5′ splice site mutation in the *IKBKAP* gene and promoted U1 snRNP recognition only to the mutated 5′ splice site (and not the wild-type 5′ splice site). Our results show that tissue-specific expression of RBM24 can explain the neuron-specific aberrant splicing of *IKBKAP* exon 20 in familial dysautonomia, and that ectopic expression of RBM24 in neuronal tissue could be a novel therapeutic target of the disease.

Keywords: RBM24; U1 snRNP; familial dysautonomia

INTRODUCTION

One-third of all disease-causing mutations have been estimated to alter pre-mRNA splicing (Lim et al. 2011; Sterne-Weiler et al. 2011; Singh and Cooper 2012). These mutations can be classified into *cis*-acting and *trans*-acting mutations and nucleotide repeat expansions (Daguenet et al. 2015). Among them, the *cis*-acting mutations can be found in 5′ donor and 3′ acceptor splice sites, polypyrimidine tract, branch point, and splicing enhancer and silencer sequences. Diseases with tissue-specific splicing defects can be expected to have mutations in splicing enhancer and silencer sequences, where the tissue-specific splicing factor would bind or lose binding and exert tissue-specific aberrant splicing. Mutations near the exon–intron boundaries would involve core splicing factors that are ubiquitously expressed, and tissue-specific effects would depend on transcriptional expression of the gene. Thus, the 5′ splice site mutation found in the *inhibitor of κ light polypeptide gene enhancer in B cells, kinase complex-associated protein* (*IKBKAP*) gene in familial dysautonomia is

[8]Present address: Department of Pharmaceutical Sciences, Fukuoka University, Fukuoka 814-0180, Japan
[9]Present address: Frontier Research Core for Life Sciences, University of Toyama, Toyama 930-0194, Japan
[10]Present address: Institute for Genetic Medicine, Hokkaido University, Sapporo 060-0815, Japan

Abbreviations: EMSA, electromobility shift assay; FD, familial dysautonomia; FGFR, fibroblast growth factor receptor; IKBKAP, inhibitor of κ light polypeptide gene enhancer in B cells, kinase complex-associated protein; IP, immunoprecipitation; RBPs, RNA-binding proteins; RF, red fluorescent protein; SPREADD, splicing reporter assay for disease genes with dual color; TAE, Tris–acetate–EDTA; TBE, Tris–borate–EDTA

Corresponding authors: hagiwara.masatoshi.8c@kyoto-u.ac.jp, akataoka@mail.ecc.u-tokyo.ac.jp

Article is online at http://www.rnajournal.org/cgi/doi/10.1261/rna.059428.116.

exceptional in that the resulting aberrantly spliced mRNA product is found in a tissue-specific manner (Cuajungco et al. 2003) in spite of the mutation residing at the 5′ splice site, and despite the original ubiquitous expression of the *IKBKAP* gene.

The molecular basis underlying tissue-specific aberrant splicing in familial dysautonomia (FD), an autosomal-recessive disorder involved in the development and survival of sensory, sympathetic, and parasympathetic neurons (Riley et al. 1949), has not been elucidated. The major FD haplotype was mapped to the *IKBKAP* gene with a T to C transition in the donor splice site of intron 20, resulting in aberrant exon skipping of exon 20. This homozygous FD mutation (IVS20 +6T>C) is found in almost all FD patients (Anderson et al. 2001; Slaugenhaupt et al. 2001). Despite the homozygous nature of the mutation, tissue-specific normal splicing of the *IKBKAP*-FD mutation is found in organs such as lymphoblast cell lines, tonsil, spleen, intercostal nerve, and skeletal muscle (Cuajungco et al. 2003). Tissue-specific alternative splicing due to genetic variations in monogenic diseases has been reported in various reports, but the *IKBKAP*-FD mutation is notable for its close genotype–phenotype correlation due to the high penetrance of the genetic variation. Thus, therapeutic control of FD-associated aberrant splicing is more beneficial for the FD patients and gives us clues for tackling tissue-specific splicing of the variations in other diseases.

Numerous compounds have been identified to correct the aberrant splicing of the *IKBKAP*-FD mutation (Anderson et al. 2003a,b; Hims et al. 2007a; Keren et al. 2010; Lee et al. 2012; Liu et al. 2013; Yoshida et al. 2015), but the splicing factors involved in tissue-specific aberrant splicing have not been uncovered (Cuajungco et al. 2003; Daguenet et al. 2015). We were motivated to find such splicing factors because they may (i) explain the peculiar tissue-specific aberrant splicing of *IKBKAP* exon 20 due to the FD mutation, (ii) reveal a novel mechanism in tissue-specific splicing, and (iii) elucidate splicing factors that can be a novel therapeutic target of familial dysautonomia.

Various strategies have been utilized to identify RNA-binding proteins (RBPs) that regulate splicing. Early studies used fractionation procedures (Krainer and Maniatis 1985; Krainer et al. 1990; Mayeda and Krainer 1992), fractionation combined with RNA affinity purification (Siebel et al. 1994), RNA covalently coupled with agarose (Caputi et al. 1999), and RNA with binding sequences for the MS2 phage coat protein (Zhou et al. 2002). RNAs incorporated with 5′-biotinylated RNA take advantage of the high affinity interaction of biotin and streptavidin and are useful for identifying the RBPs that regulate the splicing of specific genes (Hui et al. 2003). In addition to these approaches, genetic screens of the nematode *Caenorhabditis elegans* also have been shown as powerful tools for identifying RBPs that regulate splicing (Lundquist et al. 1996). We have constructed a multicolor fluorescence splicing reporter that reflects the tissue-specific alternative splicing of the *FGFR (fibroblast growth factor receptor)* gene, and succeeded in identifying the RBFOX protein, ASD-1, and the muscle-specific RNA-binding protein, SUP-12, as the tissue-specific regulators of the *FGFR* gene, egl-15 (Kuroyanagi et al. 2007; Ohno et al. 2012). Structural analysis revealed that the two RNA-binding proteins coordinately interact with a 5′-UGCAUGGUGUGC-3′ stretch and cooperatively regulate the muscle-specific alternative splicing (Kuwasako et al. 2014). SUP-12 is an evolutionally conserved member of the SUP-12–RBM24–RBM38 family of proteins (Braunschweig et al. 2013), and RBM24 was recently reported as a major enhancer of muscle-specific alternative splicing through binding to intronic splicing enhancer elements in mice (Yang et al. 2014). This multicolor fluorescence splicing reporter has been applied to the mammalian system (Takeuchi et al. 2010), making it possible to screen mutations of aberrant splicing of genes in genetic diseases for therapeutic compounds or effective RNA-binding proteins. A genomic fragment containing the wild-type and mutated sequence and spanning exon 19 to exon 21 of the human *IKBKAP* gene was cloned upstream of RFP and EGFP so that the exon-skipped mRNA was in-frame with RFP, and the exon-included mRNA was in-frame with EGFP. Thus, the reporter could easily detect alternative splicing by fluorescence—exon skipping as red and exon inclusion as green. Such splicing reporters have been constructed by inserting the entire exon and intron sequences to recapitulate the endogenous aberrant splicing as close as possible, which we named SPREADD (splicing reporter assay for disease genes with dual-color) (Yoshida et al. 2015). In this paper, we identified RBM24, using a combination of SPREADD and our focused RBPs cDNA library, as the tissue-specific regulator of FD-related aberrant splicing of *IKBKAP* exon 20 that improves U1 snRNP recognition of the 5′ splice site only in the FD-mutated context.

RESULTS

A focused screening approach using SPREADD

We have developed a dual-color splicing reporter system by inserting a target gene fragment fused downstream from the CAGGS promoter and a GST cDNA, and upstream of red fluorescent protein (RFP) and GFP cDNAs in tandem with different open reading frames (Kuroyanagi et al. 2010; Takeuchi et al. 2010). This is a powerful system that can detect alternative splicing in living cells by observation and thus is suitable for high-throughput screening. We have applied this method, which we named SPREADD, to analyze the mutations of genetic diseases by inserting the affected exon with whole lengths of adjacent introns in between partial lengths of the upstream/downstream exons from the gene of interest. Using a SPREADD reporter of familial dysautonomia (FD), we have reported a promising compound that corrects the aberrant splicing of the *IKBKAP* exon 20 found in FD patients due to the intronic 5′ splice site mutation (IVS20+6T>C) (Yoshida et al. 2015). With this reporter system, the

normal-type splicing, including exon 20, leads to expression of a GFP fusion protein, whereas FD-type abnormal splicing, which skips exon 20, results in the production of an RFP fusion protein (Yoshida et al. 2015). Here, we combined this powerful splicing reporter system with a total of 125 expression vectors of various RNA-binding proteins (Supplemental Table S1) to identify the splicing regulator(s) that suppresses FD-type exon 20 skipping (Fig. 1A). This system allows the researcher to distinguish the splicing patterns occurring in the cells by simply checking the fluorescent color observed under the microscope. Twenty-four hours after transfecting HeLa cells with this FD-splicing reporter, we investigated the percentage of GFP-dominant cells out of total cells using a Cellomics Array scan. Cotransfection of some of these cDNAs with the FD-splicing reporter dramatically enhanced the GFP signal in HeLa cells. The top three scores, above the cutoff, were that of three cDNAs: 47.45 for Rbm24 (Miyamoto et al. 2009; Xu et al. 2009; Yang et al. 2014); 37.78 for Rbm38, a paralog of Rbm24 (Shu et al. 2006; Miyamoto et al. 2009; Warzecha et al. 2009; Heinicke et al. 2013); and 21.66 for Sfpq/Psf (Patton et al. 1993) (Fig. 1B; Supplemental Table S2). The change of fluorescent color of the FD-splicing reporter by these three cDNAs is shown in Figure 1C. Semiquantitative RT-PCR confirmed that overexpression of the selected cDNAs enhanced the production of the normal-type spliced product correlating with the results of SPREADD (Fig. 1D, lanes 6–11), whereas transfection of the FD-splicing reporter with an empty vector or the FD-splicing reporter alone exclusively generated the FD-type exon 20-skipped product (Fig. 1D, lanes 3–5). Because Rbm24 is known to be differentially expressed among tissues (Miyamoto et al. 2009; Yang et al. 2014), these results gave us the notion that they might be involved in the tissue-specific regulation of *IKBKAP* exon 20 FD-type splicing.

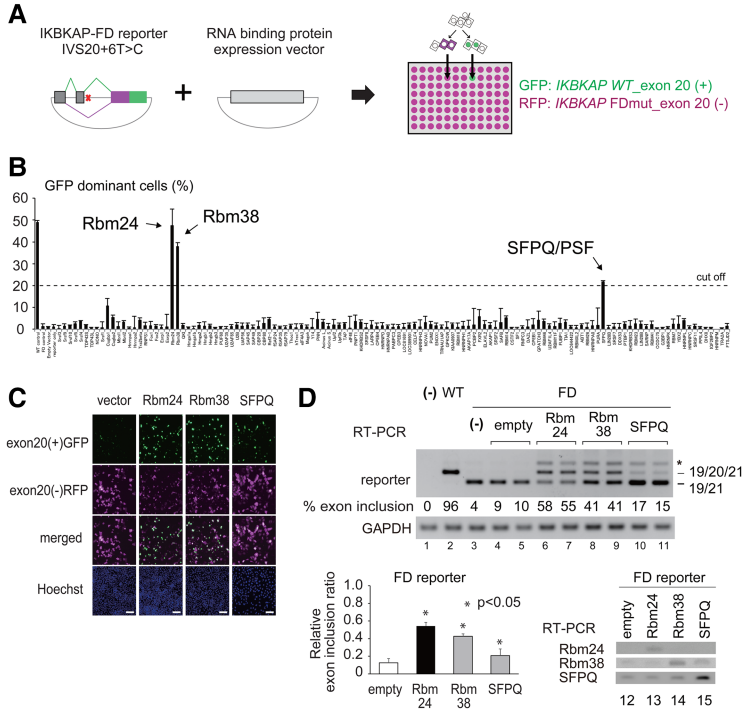

FIGURE 1. Identification of splicing regulators that correct FD-type aberrant splicing. (*A*) Strategy of high-throughput analysis for the identification of splicing regulator candidates that correct FD-type aberrant splicing. (*B*) The effect of overexpressing human and mouse RNA-binding proteins on splicing of *IKBKAP*-FD splicing reporter. The score represents the percentage of GFP-dominant cells out of total cells in three independent experiments. (*C*) Microscopic analysis of HeLa cells transfected with *IKBKAP*-FD splicing reporter and the candidate cDNAs. White scale bar, 100 µm. (*D*) RT-PCR analysis of mRNAs derived from HeLa cells transfected with the candidate RNA-binding protein cDNAs and the *IKBKAP*-FD splicing reporter (in duplicate). Bands corresponding to mRNAs of *IKBKAP* exon 20 included and excluded are indicated as 19/20/21 and 19/21, respectively. Percent of exon inclusion = inclusion/(exclusion + inclusion). Asterisk indicates a product that corresponds to a hybrid of 19/20/21-GFP and 19/21-RFP, each DNA strand from either template. The graph at *lower left* is quantification (Image J) of % exon inclusion of the FD reporter of three independent experiments. Expression of each candidate was checked by semiquantitative RT-PCR (*lower right*).

Mechanism of RBM24-induced FD-type exon skipping

We purified Flag-tagged RBM24 (Fig. 2A) using HEK293T cells and confirmed its functionality in our in vitro splicing assay (Yoshida et al. 2015). CDC-*IKBKAP*-Ex20 FD pre-mRNA is a pre-mRNA with *IKBKAP* exon 20 and a flanking intron sequence inserted in between sequence derived from chicken δ-crystallin pre-mRNA, a conventionally utilized pre-mRNA for in vitro splicing (Kataoka et al. 2000). The efficiency of in vitro splicing using HeLa nuclear extracts is limited in this type of procedure for a heterologous manner due to the stability of pre-mRNA. Importantly, this heterologous pre-mRNA recapitulates the endogenous splicing of the target exon, which we have shown in our previous report (Yoshida et al. 2015). Flag-tagged RBM24-induced exon inclusion of CDC-*IKBKAP*-Ex20 FD pre-mRNA (Fig. 2B, lanes 7–9 and 15–17) compared with CDC-*IKBKAP*-Ex20 WT pre-mRNA (Fig. 2B, lanes 3–5 and 11–13). To gain insight into the mechanism through which RBM24 exerts its function, we added increasing amounts of Flag-tagged RBM24 to a fixed amount of the core splicing factor, and we purified U1 snRNP (Fig. 2C; Kastner and Lührmann 1989) in RNA-EMSA experiments with a U1 snRNP-5′ splice site binding condition. The proportions of bisacrylamide/acrylamide for the nondenaturing gel were 1:79 to electrophorese the large purified U1 snRNP (Fig. 2C). The 5′ splice site of the *IKBKAP*

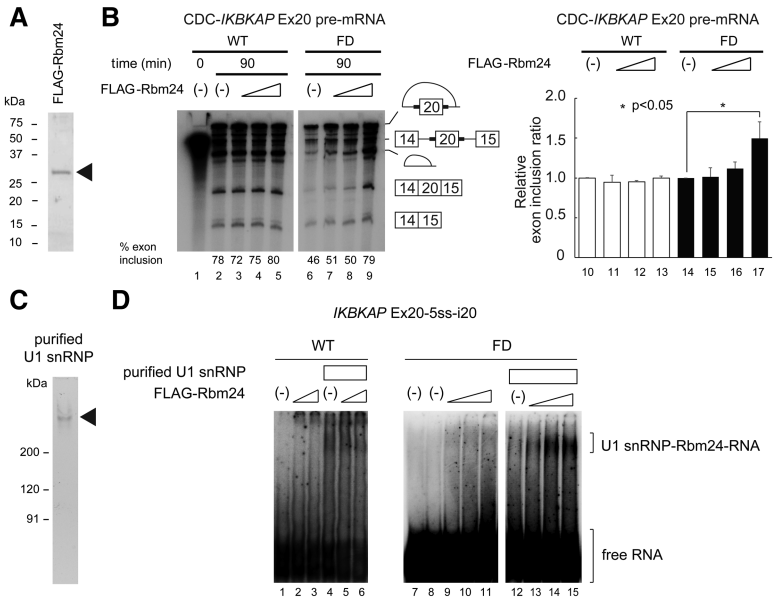

FIGURE 2. Mechanism of RBM24-induced exon inclusion of FD-type splicing. (*A*) Coomassie staining of Flag-tag RBM24 (375 ng). (*B*) In vitro splicing analysis of ^{32}P-labeled CDC-*IKBKAP*-Ex20 FD pre-mRNA with increasing amounts of Flag-tag RBM24 (9.4, 18.8, 37.5 ng [triangle]). The bold lines indicated in the splicing intermediates on the *right* side are sequence derived from *IKBKAP* exon 20 and 150 nt of upstream and downstream flanking introns. The graph on the *right* shows quantification (Image J) of three independent experiments. (*C*) Coomassie staining of purified U1 snRNP (282 ng). (*D*) RNA-EMSA of ^{32}P-labeled *IKBKAP*-Ex20–5ssFD-i20 RNA and Flag-tag RBM24 in the presence of purified U1 snRNP (282 ng). Gel composition (5% PAGE, bisacrylamide/acrylamide = 1:79) suitable for U1 snRNP binding was used.

exon 20 harboring the FD mutation is known to reduce stable base-pairing with U1 snRNP (Ibrahim et al. 2007). As shown in Figure 2D, purified U1 snRNP exhibited poor binding to the FD mutated ^{32}P-*IKBKAP*-Ex20 5ssFD-i20 RNA probe (Fig. 2D, lane 12). Increasing amounts of Flag-tagged RBM24 improved the binding of U1 snRNP to the FD mutated 5′ splice site (Fig. 2D, cf. lanes 13–15 and lane 12). Importantly, only RBM24, U1 snRNP, and radiolabeled RNA were present in the reaction, which indicated that RBM24 per se could facilitate U1 snRNP binding to the FD mutated 5′ splice site. The U1 snRNP binding to the wild-type ^{32}P-*IKBKAP*-Ex20 was not enhanced by RBM24 (Fig. 2D, lanes 4–6), suggesting that the affinity of the wild-type 5′ splice site of *IKBKAP* exon 20 for U1 snRNP was strong enough due to the sequence of the wild-type 5′ splice site. RBM24-induced exon inclusion of *IKBKAP* exon 20 was mediated by improving U1 snRNP-5′ splice site recognition of the weak FD-mutated 5′ splice site, a mechanism that can be applied to other genes where RBM24 is known to bind to intronic splicing enhancer (ISE) elements near weak 5′ splice sites (Yang et al. 2014).

RBM24 functions through an intronic splicing element

Because RBM24 is known to bind to intronic splicing enhancer (ISE) elements (Yang et al. 2014), we constructed deletion mutants in the upstream and downstream intron of exon 20 in the FD reporter (Fig. 3A). These deletions were screened by RBM24 for its ability to alter FD-type exon-skipping of each deletion in the FD reporter. The positional relationship of the FD mutation and sequence deleted in i20d1 and i20d2 are shown in Figure 3B. None of the intronic deletions upstream of exon 20 showed an effect, whereas the first deletion downstream from exon 20 (i20-d1) exhibited a reduction in FD-type exon-skipping and an increase in RBM24-induced normal exon inclusion, judged by microscopic images (Fig. 3C) and confirmed by RT-PCR (Fig. 3D). The deleted reporter (i20-d1) attenuated FD-type exon-skipping, which then was restored in i20-d2 (Fig. 3C, upper panels; Fig. 3D, lanes 1, 3, 5). This implied the existence of a negative splicing factor binding to the IVS20+13–29 element. When we expressed Rbm24 with these FD reporters (non-del., i20-d1, and i20-d2 deletions), there was a clear induction of exon inclusion for non-del. and i20-d2, but not for i20-d1 (Fig. 3C, lower panels; Fig. 3D, lanes 2, 4, 6), that was confirmed in three independent experiments (Fig. 3D, lower graph). We also confirmed that Flag-tagged RBM24 binds to the IVS20+13–29 element in RNA-EMSA experiments (Fig. 3E). The proportion of bisacrylamide/acrylamide for nondenaturing gel used in the RNA-EMSA of Figure 3E was 1:29, which differed from the nondenaturing gel of Figure 2D due to the small size of RBM24 and the need for better resolution. G to C substitutions in the IVS20+13–29 element abolished RBM24-binding to RNA harboring the wild-type 5′ splice site (Fig. 3E, cf. lanes 2–4 with lanes 6–8) or FD-mutant 5′ splice site (Fig. 3E, compare lanes 10–12 with lanes 14–16), which is reminiscent of SUP-12, a member of the same SUP-12-RBM24-RBM38 family (Kuwasako et al. 2014).

Endogenous RBM24 induces normal-type exon inclusion from *IKBKAP*-FD pre-mRNA

Because RBM24 is known as a major regulator of muscle-specific alternative splicing (Yang et al. 2014), we checked the expression of Rbm24 mRNA in various human tissues by semiquantitative RT-PCR (Fig. 4A). The heart and skeletal muscle had the strongest expression (Fig. 4A, lanes 4, 5), whereas brain showed almost no expression (Fig. 4A, lane 1). In comparison to Rbm24, the distribution of *IKBKAP* mRNA expression, also judged by semiquantitative RT-PCR, is rather ubiquitous (Supplemental Fig. S1). RBM38

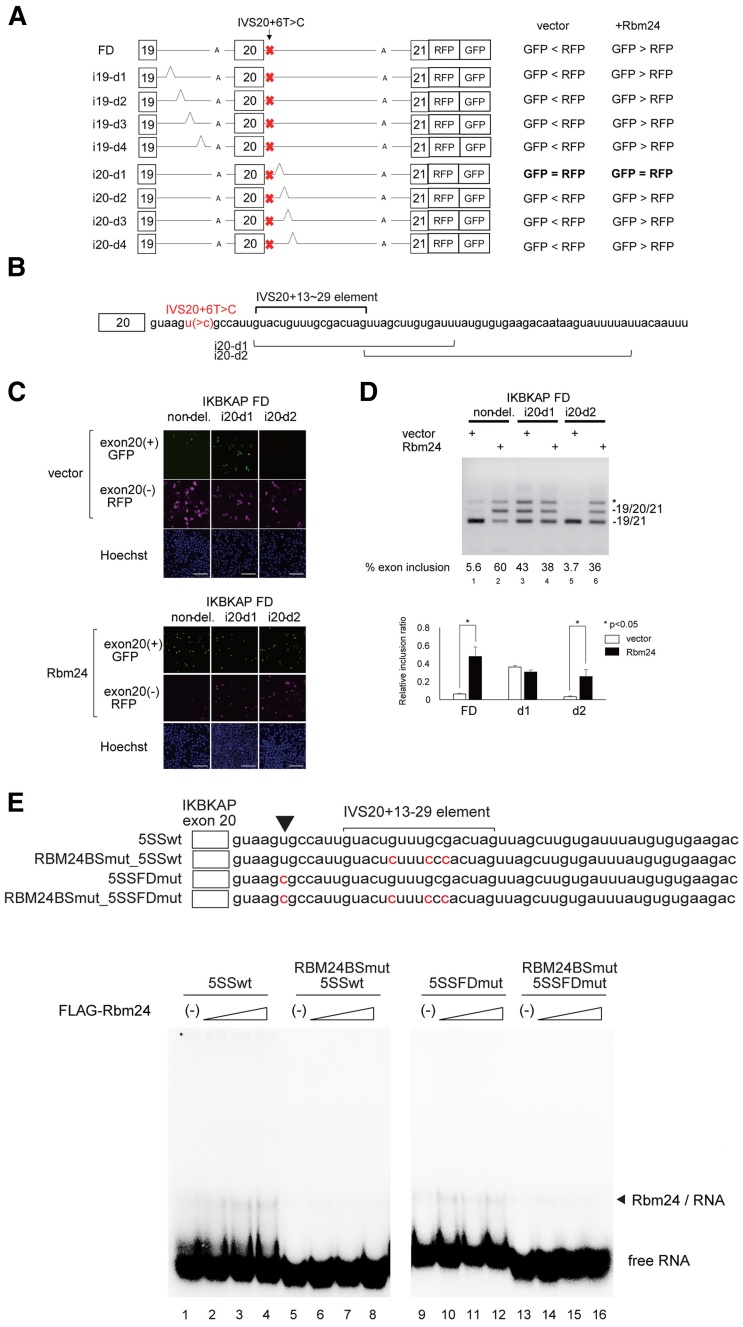

FIGURE 3. IVS20+13–29 element is important for Rbm24-induced normal-type splicing of the *IKBKAP*-FD reporter. (*A*) Deletions used to screen the target element of RBM24 (*left* side of panel). Results of SPREADD for each deletion without Rbm24 cotransfection (vector) and with Rbm24 cotransfection (+Rbm24) are shown on *right* side. Comparison of expression level is shown as equation. (*B*) Schematic representation of i20-d1 and i20-d2 deletions of the I*KBKAP*-FD splicing reporter. The IVS20+13–29 element, deleted region of i20-d1 and i20-d2 are indicated by parentheses. (*C*) Microscopic analysis of HeLa cells transfected with the *IKBKAP*-FD splicing reporter, *IKBKAP*-FD i20d1 splicing reporter, and *IKBKAP*-FD i20d1 splicing reporter without and with Rbm24. White scale bar indicates 100 µm. (*D*) Semiquantitative RT-PCR analyses of HeLa cells transfected with the *IKBKAP*-FD splicing reporter, *IKBKAP*-FD i20d1 splicing reporter, and *IKBKAP*-FD i20d1 splicing reporter without and with Rbm24 (*upper* panel). Graphic results of three independent experiments of the *upper* panel quantified by Image J (*lower* panel). (*E*) RNA-EMSA of ^{32}P-labeled *IKBKAP*-Ex20-5ss-i20 RNA and Flag-tag RBM24. Sequence of 5SSwt, RBM24BSmut_5SSwt, 5SSFDmut, and RBM24BSmut_5SSwt are depicted in *upper* panel with the FD mutation and mutation of the GU-rich region shown in red letters. Normal gel composition (5% PAGE, bisacrylamide/acrylamide = 1:29) was used.

also showed ubiquitous expression with the strongest expression in leukocytes (Supplemental Fig. S1). Because it is known that Rbm24 expression is induced upon myogenic differentiation (Miyamoto et al. 2009), we wanted to confirm whether induced endogenous expression of Rbm24 in C2C12 muscle cells could suppress FD-type exon 20 skipping. For this purpose, C2C12 cells that stably expressed the FD splicing reporter were generated. After changing the medium to the differentiating medium for 2 d, the GFP signal became stronger with cells beginning to form myotubes (Supplemental Fig. S2). Among the myotubes, clusters of GFP signals from cells with multiple nuclei emerged (Fig. 4B, upper panel; Supplemental Fig. S2). Induced differentiation accompanied by Rbm24 expression was verified by immunofluorescence (Fig. 4B, upper panel), showing that induced expression of endogenous RBM24 can induce exon inclusion of the FD-splicing reporter in differentiated muscle cells. Figure 4B, lower left panel verifies differentiation by RT-PCR of myosin heavy chain type 3 along with induced Rbm24 expression. The extent of exon inclusion of the FD reporter was compared with immunofluorescence of endogenous Rbm24 in these cells. As shown in the lower right panel of Figure 4B, GFP/(RFP + GFP) ratio had a strong correlation with the immunofluorescence level of Rbm24 ($r = 0.72$).

To verify that endogenous RBM24 could induce exon inclusion of the FD-splicing reporter, we conducted a knockdown of RBM24 in primary mouse muscle cells simultaneously transiently transfected with the FD-splicing reporter. Rbm24 knockdown in primary mouse muscle cells showed a clear reduction of the exon inclusion ratio of the FD-splicing reporter along with reduced RBM24 protein expression (Fig. 4C). The knockdown was assessed with two other different siRNAs with distinct levels of Rbm24 knockdown. The level of Rbm24 expression by three different siRNA knockdowns varied but correlated well with the exon-inclusion ratio of the FD-splicing reporter ($r = 0.91$) (Supplemental Fig. S3).

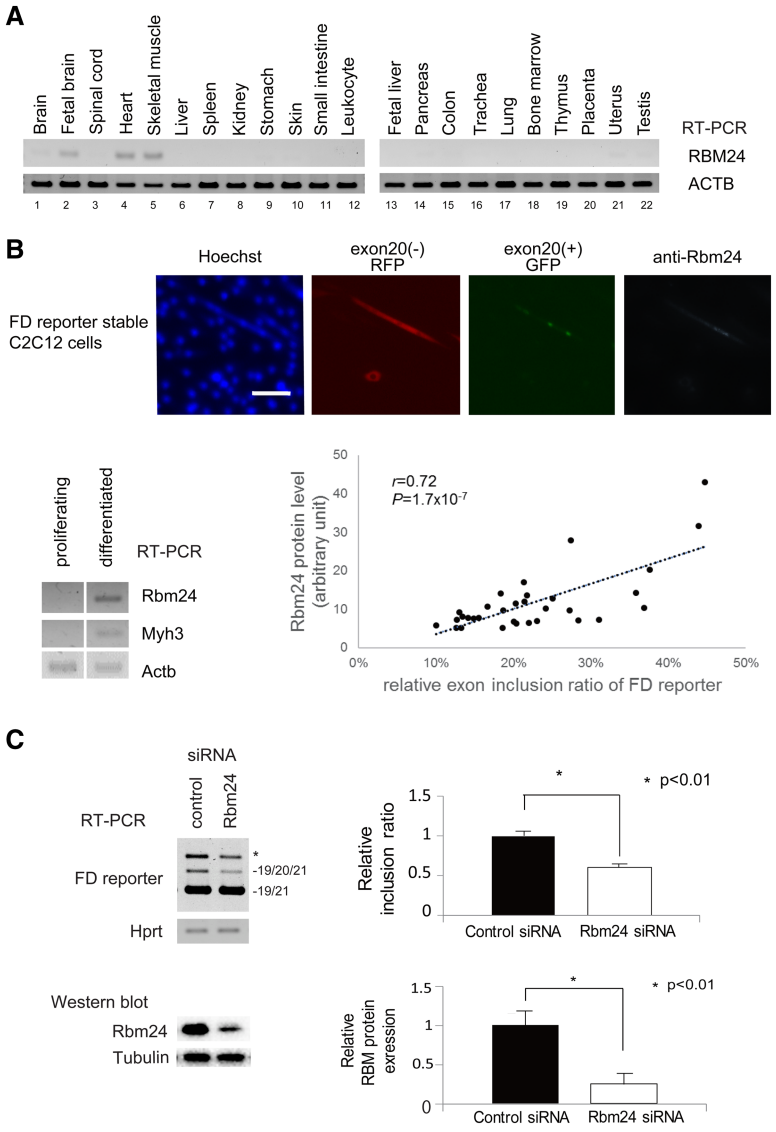

FIGURE 4. Muscle-specific expression and function of Rbm24. (*A*) Muscle-specific expression of RBM24. Semiquantitative RT-PCR of RBM24 and ACTB using a human total RNA panel. (*B*) Microscopic analysis of C2C12 cells stably transfected with the *IKBKAP*-FD reporter and differentiation induced to visualize exon inclusion [exon20(+)GFP] by endogenous RBM24 expression (anti-RBM24) (*upper* panels) (white scale bar, 50 µm). Expression of Rbm24, Myh3, and ActB in C2C12 cells stably expressed of the *IKBKAP*-FD reporter (*left* panels) to confirm induced Rbm24 expression upon muscle differentiation (Myhc3: Myosin heavy chain 3, Actb: β-actin). *Lower right* graph indicates the correlation of exon inclusion ratio [GFP/(RFP+GFP)] and strength of anti-RBM24 positivity. (*C*) siRNA knockdown of Rbm24 in primary culture mouse muscle cells attenuate exon 20 inclusion of the FD reporter. *Upper left* panel shows semiquantitative RT-PCR of the FD splicing reporter. Three independent experiments were performed, and results are shown as a graph at the *upper right*. *Lower left* panel is an immunoblot of the RBM24 protein of these primary mouse muscle cells knocked down by Rbm24. Three independent experiments were performed and results are shown as a graph at the *lower right*.

Ectopic RBM24 induces normal-type splicing of the *IKBKAP*-FD reporter in neuronal cells and the endogenous *IKBKAP*-FD-mutated gene in FD-patient fibroblasts

We next tested the ability of Rbm24 to induce normal-type exon inclusion of the FD-splicing reporter in neuronal cells. We transfected a primary culture of mouse neurons with the *IKBKAP*-FD-splicing reporter along with the Rbm24 expression vector, resulting in clear induction of normal-type exon inclusion, as observed under the microscope (Fig. 5A). The same procedure was also performed using neural stem cells (Fig. 5B) with similar results. Because the transfection efficiency of these primary cultured neuronal cells was poor, we verified splicing by RT-PCR and received comparable results to the primary cultured mouse neuronal cells and neural stem cells, showing that RBM24 induced normal-type exon inclusion of the FD-splicing reporter and that RBM24 was properly expressed (Fig. 5A,B, right panels). It can be also noticed here that higher levels of anti-RBM24 staining correlated well with the strength of the GFP signal (Exon20+) (Fig. 5A,B, lower panels).

Finally, because we used only reporter *IKBKAP* pre-mRNAs throughout this report, we tested the influence of RBM24 on the endogenously exon-skipped *IKBKAP* exon 20 in mutated FD-patient fibroblasts. Carrier fibroblast cells, which harbor the mutation on a single allele but have no symptoms of familial dysautonomia, showed almost no exon-skipping (Fig. 5C, lanes 1,2,3), whereas FD-patient fibroblast cells #42 and #50 showed skipping of *IKBKAP* exon 20, and both were corrected by RBM24 (Fig. 5C, cf. lanes 4 and 5 for FD#42, and lanes 7 and 8 for FD#50). Rbm38 did not show such consistent effects as RBM24 (Fig. 5C, cf. lanes 4 and 6 for FD#42, and lanes 7 and 9 for FD#50).

Taken together, RBM24 functions as a tissue-specific cryptic splicing enhancer of *IKBKAP*-FD pre-mRNA. *IKBKAP* exon 20 is not skipped in the wild-type context, even in neuronal tissue where RBM24 has almost no expression, but it is skipped in the FD-mutation context in neuronal tissue, making the IVS20 +13–29 element a cryptic splicing enhancer (Fig. 6). We showed here that tissue-specific distribution of RBM24 well explains the differential splicing pattern due to the IVS20+6T>C mutation as well as its function in promoting U1 snRNP recognition of the *IKBKAP* exon 20 5′ splice site only in the FD-mutated context. The effect of RBM24 in neuronal cells as well as

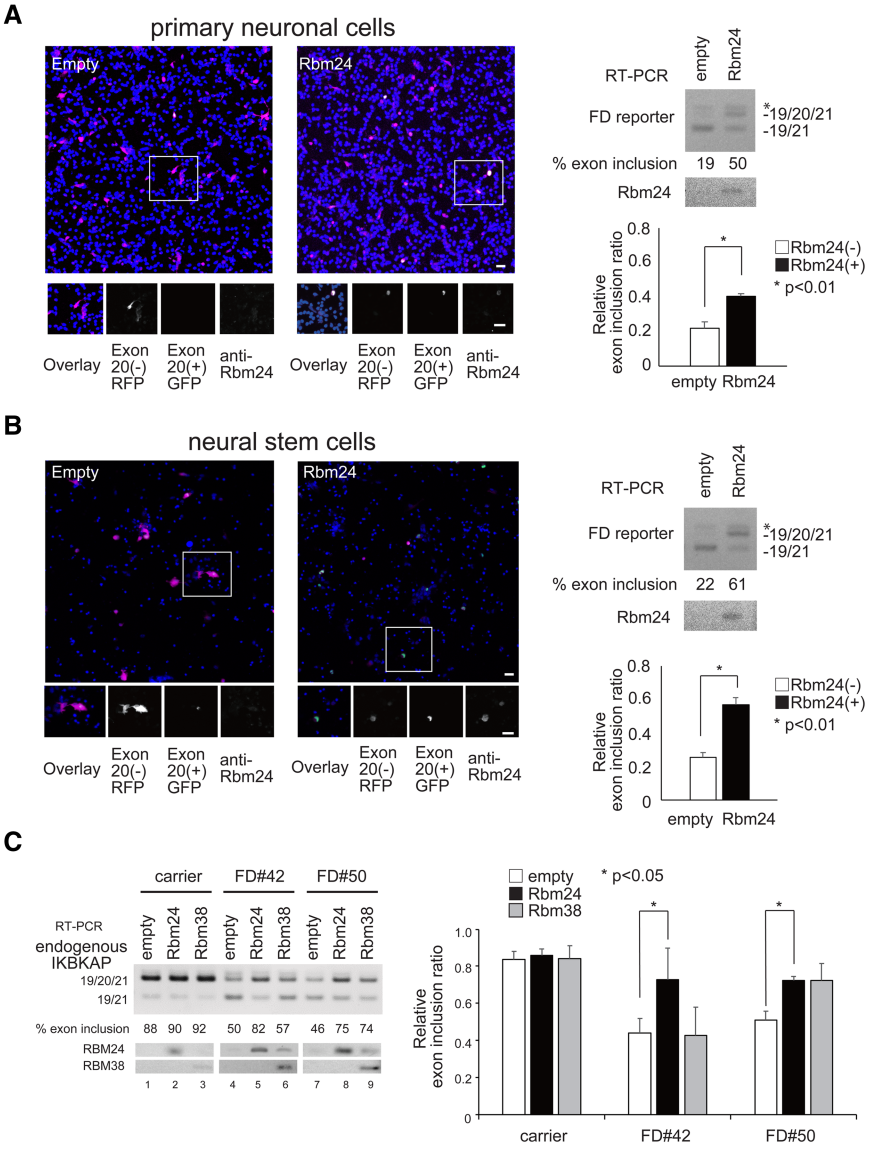

FIGURE 5. RBM24 can induce normal-type splicing of the FD splicing reporter in neuronal cells. (*A*) Microscopic analysis (*left* panels) and RT-PCR analyses (*right* panels) of FD splicing reporter using primary neuronal cells. White scale bar (*left* panels), 10 µm. (*B*) Microscopic analysis (*left* panels) and RT-PCR analyses (*right* panels) of FD splicing reporter using neural stem cells. White scale bars (*left* panels), 10 µm. (*C*) Effect of RBM24 and RBM38 on FD-patient skin fibroblasts (FD #42, FD #50). *Left* panel shows RT-PCR analyses of skin fibroblasts (carrier, FD#42, FD#50) transfected with expression vectors of Rbm24 and Rbm38. *Lower left* panels show expression of RBM24 and RBM38. *Right* graph shows quantification of RT-PCR analyses.

patients' fibroblasts implies its therapeutic potential in familial dysautonomia.

DISCUSSION

In a screen of 125 RNA-binding proteins, Rbm24 had the strongest effect on correcting the aberrant splicing of *IKBKAP* exon 20 in familial dysautonomia (FD). We used the FD splicing reporter system that we call SPREADD, a system that recapitulates aberrant splicing found in familial dysautonomia (Yoshida et al. 2015).

After careful evaluation, we found that RBM24 functions as an intronic splicing enhancer binding to an element (IVS20 +13–29) downstream from the intronic 5′ splice site mutation (IVS20+6T>C) in the *IKBKAP* gene. We showed here that RBM24 induced inclusion of endogenous *IKBKAP* exon 20 in FD patients' fibroblasts but not in carrier fibroblasts. This result was recapitulated in our splicing reporter system using muscle cells and neuronal cells. However, we were not able to test this in patients' neurons, which is a limitation of this study. The in vitro data here show the direct improvement of U1 snRNP-5′ splice site recognition by RBM24 via RNA-binding. This is the second report, to our knowledge, showing such direct evidence of improvement in U1 snRNP binding to a 5′ splice site by an intronic splicing enhancer (Förch et al. 2000).

Element (IVS20+13–29) functions as a cryptic splicing enhancer

Importantly, RBM24 induced *IKBKAP* exon 20 inclusion only in the FD-mutation context. The wild-type *IKBKAP* gene has not been documented for disruption of exon 20 inclusion in neuronal tissue where RBM24 is not expressed. Thus, RBM24 does not function for exon 20 inclusion in the wild-type context.

We have shown RBM24 does not enhance U1 snRNP binding to the wild-type 5′ splice site (Fig. 2D lanes 4–6) that may cause hyperstabilization and abrogate its function (Ohe and Mayeda 2010). The IVS20+13–29 element is a naturally silent intronic splicing enhancer, in the wild-type context, summarized as a model in Figure 6. The only other report of such an enhancer is the human *fibrinogen Bβ-chain* gene, where the mutation, IVS7+1G>T, was found to evoke the function of a naturally silent SRSF1 binding site in exon 7 (Spena et al. 2006). However, we believe such cryptic enhancer elements are not so rare and that further advances in analyzing changes in the local RNA-binding protein repertoire of splice site mutations will reveal more examples and unveil the evolutionary meaning of cryptic splicing enhancers. *IKBKAP* exon 20 is

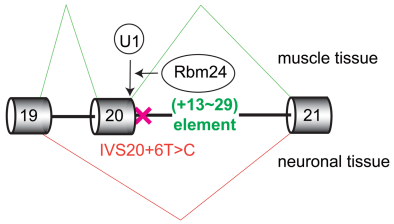

FIGURE 6. Model of the normal-type-induced splicing by RBM24 in the context of the FD mutation (IVS20+6T>C). Normal-type splicing is found in muscle tissue where RBM24 is expressed and FD-type splicing in neuronal tissue where RBM24 expression is low.

evolutionarily conserved in vertebrates, but the 5′-uguuug-3′ sequence in the IVS20+13–29 element appears after prosimians (Supplemental Fig. S4), leaving the evolutionary acquirement of the IVS20+13–29 element as another interesting issue. Additionally, the results in Figure 3C,D show that a negative splicing factor may also bind to the IVS20+13–29 element, and that RBM24 induces exon inclusion by antagonizing this negative splicing factor. More detailed future analyses will reveal the precise elements required for both negative and positive regulation, as well as characterization of this negative splicing factor.

RBM24 or element (IVS20+13–29) as a therapeutic target in familial dysautonomia

Our tissue expression data show that RBM24 is expressed in the fetal brain and down-regulated to a minute amount in the adult brain (Fig. 4A). *Ikbkap* knockout studies in mice show that it has a critical function for the maintenance of "tyrosine receptor kinase"-positive ($TrkA^+$) sensory and sympathetic neurons, not on trunk neural crest migration (George et al. 2013). Thus, ectopic expression of RBM24 in these $TrkA^+$ neurons may recover loss of autonomous and sensory neurons in FD patients. This awaits further analyses of RBM24 in neuronal development, but would be a promising therapeutic target if RBM24 is down-regulated in $TrkA^+$ cells where Ikbkap has a critical function. If the *IKBKAP* gene is aberrantly spliced in patient $TrkA^+$ cells, up-regulation or ectopic expression of RBM24 would induce normal-type *IKBKAP* alternative splicing as our data show here. Though we have not tested the ability of RBM24 to induce *IKBKAP* exon 20 inclusion in patients' neurons, we believe our results clearly show the potency of RBM24 as a therapeutic target for FD. The straightforward strategy would be to express RBM24 in neuronal tissue of FD-derived iPS cells (Lee et al. 2009) and FD-model mice (Hims et al. 2007b; Dietrich et al. 2012; Bochner et al. 2013; Morini et al. 2016) and find possibilities in therapeutic applications. An alternative would be to regulate expression of microRNAs that target RBM24. It has been reported that miR-125b targets RBM24 and that expression of miR-125b is down-regulated in the heart (Vacchi-Suzzi et al. 2013). Conversely, miR-125b is up-regulated during neuronal differentiation (Le et al. 2009; Warzecha et al. 2009). Although it remains unclear at which stage a certain phenotype of neuron RBM24 is expressed, targeting miR-125b may improve RBM24 expression and may correct FD-type splicing in FD-neuronal tissue, but this awaits further investigation.

In summary, we show here evidence of RBM24, found in a screen of RNA-binding proteins using SPREADD, regulating tissue-specific splicing of the mutant *IKBKAP* gene in familial dysautonomia. The tissue-specific RNA-binding to this element, as well as the element per se, can serve as a novel therapeutic target of this devastating disease. Our results show that mutations where core splicing factors result in weak binding can result in tissue-specific aberrant splicing due to RBPs with tissue-specific expression. In this scenario, a common mechanism may be underlying many other genetic mutations where aberrant splicing is found in affected organs. The focused RBP expression library used here would be useful in finding the factor involved and therapeutic applications that may be considered for the genetic disease.

MATERIALS AND METHODS

cDNA expression screening

We transfected HeLa cells with human *IKBKAP* splicing reporter and a cDNA library of major mammalian RNA-binding proteins (Supplemental Table S1), using TransFectin Lipid Reagent (Bio-Rad) in a 96-well plate. After 24 or 48 h, cells were washed with PBS (Nacalai Tesque) and then fixed with 4% paraformaldehyde (Nacalai Tesque) for 10 min. The fixed cells were stained for 30 min with 5 µg/mL Hoechst 33342 and 1% Triton-X 100 in PBS, then washed with PBS once to remove excess Hoechst. After staining the nucleus, cells were kept in PBS and visualized using an ArrayScan VTI (Thermo Fisher Scientific). The Compartment Analysis algorithm was used to define a primary object, apply a "nucleic and cytoplasmic" mask and quantitate GFP and RFP intensity in the mask, respectively. A primary object was defined as the nucleus by Hoechst and the "nucleic and cytoplasmic" mask was set two pixels wider from the primary object. The inside of the "nucleic and cytoplasmic" mask was quantified for GFP and RFP signals because E19/20/21-GFP proteins were predominantly distributed in the nucleus. On the other hand, E19/21-RFP proteins were mainly distributed in the cytoplasm. A GFP-dominant cell was defined as >3 SD of the mean value of GFP/RFP in control (DMSO) cells.

Plasmids, C2C12 stable transfectants of the FD-splicing reporter

We utilized the *IKBKAP* splicing reporter vectors that we previously reported (Yoshida et al. 2015). Deletions of the *IKBKAP* splicing reporter vectors (i19d1, i19d2, i19d3, i19d4, i20d1, i20d2, i20d3, i20d4) were constructed by overlap PCR using the indicated primers (Supplemental Table S3). As a first step, the 5′ portion and 3′ portion on both sides of the intended deletion were amplified separately by PCR with an overlapping sequence of 20–25 bp. As a second step,

these PCR products were combined, annealed, and amplified using primers for the full-length insert of the splicing reporter. Each PCR product was inserted into a splicing reporter with appropriate restriction enzymes. The resulting fragment was full length with the intended sequence deleted.

The dual-color jump-in FD-splicing reporter destination vector (nV68) was constructed as described below. First, a 2-nt insertion was introduced upstream of the HindIII site in pJTI Fast DEST (Invitrogen) to shift the reading frame. Then, the fragments of the pCAGGS promoter region and GFP–RFP region amplified from our splicing reporter (Yoshida et al. 2015) were inserted into the modified pJTI Fast DEST with KpnI and HindIII, respectively. The primers used for the 2-nt insertion and amplification of the fragments are described in Supplemental Table S4. The entry clones of the human *IKBKAP* genomic DNA fragment spanning exon 19 to exon 21 with the FD-mutation (IVS20+6T>C) and modified GST (Takeuchi et al. 2010) and the destination vector nV68 were recombined through its attR1 and attR2 sites to create the *IKBKAP*-FD jump-in splicing reporter (Jump-In system [Life Technologies–Invitrogen]).

C2C12 stable transfectants of the FD-splicing reporter were developed by cotransfecting the *IKBKAP* jump-in splicing reporter and pJTI PhiC31 Int vector (Invitrogen) to integrate the splicing reporter into the genome of C2C12 cells through pseudo-attP sites. Subsequent stable transfectants of the *IKBKAP*-FD jump-in splicing reporter were selected by 400 μg/mL hygromycin B. Myogenic differentiation was induced by culturing C2C12 cells stably expressing the FD-splicing reporter up to subconfluency in DMEM supplemented with 10% fetal bovine serum, and then changing to differentiating medium (DMEM supplemented with 2% horse serum) for 2 d. For evaluation of the correlation between RBM24 expression and the exon inclusion ratio of the FD reporter, overly weak signals of RFP (34 out of 84 randomly selected cells) and overly strong signals (eight out of 84 randomly selected cells) were eliminated.

Cell culture, mouse primary muscle cells and siRNA knockdown, FD-patient cells, and transfection

HeLa cells were cultured in DMEM (Nacalai Tesque) supplemented with 10% fetal bovine serum at 37°C in 5% CO_2, and transfection was performed using FuGeneHD (Promega) in 12-well dishes. Cells were cotransfected with 0.5 μg per well of the reporter plasmid and 0.5 μg per well of a plasmid expressing individual RNA-binding proteins.

Mouse primary myoblast cells were cultured by a method previously reported (Rando and Blau 1994; Tanihata et al. 2008). In brief, limbs of 10-wk-old male C57BL/6J mice (Japan CLEA Co.) were removed and dissected to remove bones. PBS was added to the muscle tissue and minced into slurry using scissors. Cells were enzymatically dissociated by 0.2% collagenase type 2 (Worthington Biochemical Corporation) and passed through an 18-gauge needle. The solution was filtered by 100-μm and 40-μm nylon mesh (Falcon, BD Biosciences). The filtrate was spun and sedimented cells were cultured in growth medium. These cells were transfected with siRNA using the commercially available Stealth siRNA technology (Invitrogen [Thermo Fisher Scientific]). An siRNA duplex that targets mouse Rbm24 (5′-CACCACACCGUACAUUGAUUACAC-3′) (Fig. 4C, siRNA and Supplemental Fig. S3, siRNA①) in the negative control medium GC #2 (Invitrogen [Thermo Fisher Scientific]) was transfected using the JetPrime transfection reagent (Polypus Transfection) in 24-well dishes coated with type I collagen (Iwaki), and then simultaneously changed to differentiation medium. The siRNA duplex used in Supplemental Figure S3 was obtained from the commercially available Silencer Select siRNA technology (Invitrogen [Thermo Fisher Scientific]): s125621 for siRNA② and s125620 for siRNA③. Control siRNA was also obtained from the same source (Invitrogen [Thermo Fisher Scientific] Cat. no. 4390846).

Fibroblast cell lines from FD patients were obtained from the National Institute of General Medical Sciences Human Genetic Mutant Cell Repository as we previously reported (Yoshida et al. 2015). The cell line nos. 50 (GM00850), 42 (GM02342), and carrier (GM04664) were cultured in DMEM supplemented with 15% (vol/vol) FBS. These FD-patient fibroblast cell lines were cotransfected as HeLa cells except that Lipofectamine 3000 (Invitrogen) was used.

Primary neuronal cultures were prepared from an embryonic 18-d-old mouse. To visualize FD-type splicing in primary neurons, the FD-splicing reporter was transfected using the calcium phosphate method at day 5 in vitro. For RT-PCR analysis, 1.5 μg of each plasmid expressing the FD reporter and RBM24 was electroporated using Nucleofector II (Lonza). Neural stem-cell cultures were prepared from an embryonic 13-d-old mouse and passaged every 3–4 d. After the third passage, cultures were used for electroporation. All animal care and use was approved by the Institutional Animal Care and Use Committee of Kyoto University Graduate School of Medicine.

Semiquantitative RT-PCR

Total RNAs were prepared from culture cells using TRIzol (Invitrogen) according to the manufacturer's instructions and treated with RNase-free DNase (RQ1; Promega). One microgram of these total RNA or 0.5 μg of human tissue total RNA (Human total RNA Master Panel II, Clontech) was reverse transcribed as follows: First-strand cDNA was synthesized using reverse transcriptase (PrimeScript RT Reagent Kit, TaKaRa Bio. Inc.) with random hexamers. Semiquantitative RT-PCR was performed with Ex Taq polymerase (TaKaRa Bio. Inc.) using an appropriate set of primers indicated in Supplemental Table S4.

Flag-tag protein purification, in vitro splicing, and RNA-EMSA

Flag-tag Rbm24 protein was purified from HEK293T cells stably transfected with Rbm24 (Flp-In T-REx293/Flag-Rbm24) using the Flp-In system (Life Technologies). Flag sequence (DYKDDDDK) was placed at the amino terminus of the protein and cloned into the pcDNA5 vector. This pcDNA5-Flag-Rbm24 expression vector and pOG44 vector (expressing Flp recombinase) were transfected into Flp-In T-Rex-293 cells and selected by medium supplemented with 100 μg/mL hygromycin and 15 μg/mL blasticidin. Two 100-mm plates of Flp-In T-REx293/Flag-Rbm24 cells were induced by tetracycline (1 μg/mL) for 24 h and harvested. The cells were washed once with PBS and 420 mM NaCl IP (immunoprecipitation) buffer (420 mM NaCl, 20 mM HEPES [pH 7.5], 1.5 mM $MgCl_2$, 0.1% NP-40) with 1% proteinase inhibitor cocktail (#25955-11, Nacalai Tesque) was added (1 mL/1.0×10^7 cells). The pellet was dispersed by pipetting and then rotated for 1 h at 4°C. After centrifugation at

15,000 rpm for 15 min at 4°C, the supernatant was collected, anti-Flag M2 Affinity Gel (Sigma-Aldrich, A2220) was added (25 µL bed volume/1×10^7 cells), and samples were rotated for three hours at 4°C. The beads were washed twice with 1 M IP buffer (1 M NaCl, 20 mM HEPES [pH 7.5], 1.5 mM $MgCl_2$, 0.1% NP-40), washed twice with 420 mM NaCl IP buffer, and washed once in general wash buffer (150 mM NaCl, 50 mM HEPES [pH 7.5]). The 3xFlag peptide was used (25 µL/1.0×10^7 cells) to elute the protein, which was dialyzed in buffer D′ (20 mM HEPES [pH 7.5], 60 mM KCl, 0.2 mM EDTA, 10% glycerol) overnight.

In vitro splicing assays were performed as previously described (Ohe and Mayeda 2010) with slight modifications. Briefly, instead of the standard protocol where all components are mixed on ice, the reaction mixture was mixed in the following order and incubated at 30°C prior to addition of nuclear extract: First, the Flag protein was mixed with the probe and the splicing mixture was added and incubated at 30°C for 5 min. At this point, the concentrations of Mg and ATP were 7.8 mM and 1.25 mM, respectively. Then HeLa nuclear extract and PVA were added to start the splicing reaction at 30°C in final concentrations of Mg and ATP at 3.2 and 0.5 mM, respectively.

RNA-electromobility shift assays (RNA-EMSA) of U1 snRNP were performed in a binding buffer suited for U1 snRNP binding, as previously described (Ohe and Mayeda 2010) and analyzed by 5% PAGE (acrylamide:bisacrylamide ratio = 79:1 [wt/wt]) at 4°C using 0.5× Tris–borate–EDTA (TBE) buffer for Figure 2C.

RNA-EMSA for RBM24 (Fig. 3E) was performed with minor modifications mimicking the in vitro splicing reaction: Flag protein was mixed with the probe, which was denatured briefly at 65°C, and rapidly cooled to avoid multiple species of free RNA. The splicing mixture was added and incubated at 30°C for 5 min (the concentration of Mg was 7.8 mM and ATP was 1.25 mM at this point); then a modified binding buffer (3 mM $MgCl_2$, 50 mM KCl, 20 mM HEPES [pH 7.5], 0.1 mM EDTA, 10% glycerol) was added and incubated at room temperature for an additional 15 min. The bound complexes were analyzed by 5% PAGE (acrylamide:bisacrylamide ratio = 29:1 [wt/wt]) at room temperature using 0.25× Tris–acetate–EDTA (TAE) buffer. Dried gels of RNA-EMSA and in vitro splicing were visualized using a Typhoon 9600 imager (GE Healthcare).

The *IKBKAP* exon 20-5ssFD-i20 probe was transcribed from a PCR product containing the T7 promoter (Fig. 3E). The RNA sequence for the *IKBKAP*-Ex20-5ssFD-i20 probe is 5′-GAAGCUU CGGAAGUGGUUGGACAAguaagcgccauuguacuguuugcgacuaguua gcuugugauuuauguguugaagac-3′, and for the *IKBKAP* exon 20-5ssFD-i20-d1 probe it is 5′- GAAGCUUCGGAAGUGGUUGGACAAguaag cgccauuauuuuauuacaauuucgagaacuuaaaauuaugaaaagcccuc-3′.

SUPPLEMENTAL MATERIAL

Supplemental material is available for this article.

ACKNOWLEDGMENTS

We thank Dr. Jun Tanihata and Dr. Shinichi Takeda at the Department of Molecular Therapy, National Institute of Neuroscience, National Center of Neurology and Psychiatry (Tokyo, Japan) for their assistance in mouse primary myoblast cell culture. We are grateful to Ruis J. Philip (Amgen Scholars Program 2015) and James F. Meng (Kyoto University Laboratory Visiting Program International Student Internship 2015 [for Foreign Students]) for experimental assistance, helpful discussions, and comments on this manuscript. We thank Keiko Hayashi and Takafumi Yamasaki for experimental assistance. We thank Enago (www.enago.jp) for the English language review. We also thank the Radioisotope Research Center and the Medical Support Center of Kyoto University and Radioisotope Center at Fukuoka University for instrumental support. All authors have read and approved the manuscript. This work was supported by Grants-in-Aid for Scientific Research (15H05721 to M.H., 23112706 to N.K., and 15K10050 to K.O.); Research Program of Innovative Cell Biology (231006 to M.H.); National Institute of Biomedical Innovation (NIBIO, 241011 to M.H.); and CREST of Japan Science and Technology Agency (JST) (231038 to M.H.). The funders had no role in study design, data collection and analysis, decision to publish, or preparation of the manuscript.

Received October 6, 2016; accepted May 25, 2017.

REFERENCES

Anderson SL, Coli R, Daly IW, Kichula EA, Rork MJ, Volpi SA, Ekstein J, Rubin BY. 2001. Familial dysautonomia is caused by mutations of the IKAP gene. *Am J Hum Genet* **68:** 753–758.

Anderson SL, Qiu J, Rubin BY. 2003a. EGCG corrects aberrant splicing of IKAP mRNA in cells from patients with familial dysautonomia. *Biochem Biophys Res Commun* **310:** 627–633.

Anderson SL, Qiu J, Rubin BY. 2003b. Tocotrienols induce *IKBKAP* expression: a possible therapy for familial dysautonomia. *Biochem Biophys Res Commun* **306:** 303–309.

Bochner R, Ziv Y, Zeevi D, Donyo M, Abraham L, Ashery-Padan R, Ast G. 2013. Phosphatidylserine increases IKBKAP levels in a humanized knock-in IKBKAP mouse model. *Hum Mol Genet* **22:** 2785–2794.

Braunschweig U, Gueroussov S, Plocik AM, Graveley BR, Blencowe BJ. 2013. Dynamic integration of splicing within gene regulatory pathways. *Cell* **152:** 1252–1269.

Caputi M, Mayeda A, Krainer AR, Zahler AM. 1999. hnRNP A/B proteins are required for inhibition of HIV-1 pre-mRNA splicing. *EMBO J* **18:** 4060–4067.

Cuajungco MP, Leyne M, Mull J, Gill SP, Lu W, Zagzag D, Axelrod FB, Maayan C, Gusella JF, Slaugenhaupt SA. 2003. Tissue-specific reduction in splicing efficiency of IKBKAP due to the major mutation associated with familial dysautonomia. *Am J Hum Genet* **72:** 749–758.

Daguenet E, Dujardin G, Valcárcel J. 2015. The pathogenicity of splicing defects: mechanistic insights into pre-mRNA processing inform novel therapeutic approaches. *EMBO Rep* **16:** 1640–1655.

Dietrich P, Alli S, Shanmugasundaram R, Dragatsis I. 2012. IKAP expression levels modulate disease severity in a mouse model of familial dysautonomia. *Hum Mol Genet* **21:** 5078–5090.

Förch P, Puig O, Kedersha N, Martínez C, Granneman S, Séraphin B, Anderson P, Valcárcel J. 2000. The apoptosis-promoting factor TIA-1 is a regulator of alternative pre-mRNA splicing. *Mol Cell* **6:** 1089–1098.

George L, Chaverra M, Wolfe L, Thorne J, Close-Davis M, Eibs A, Riojas V, Grindeland A, Orr M, Carlson GA, et al. 2013. Familial dysautonomia model reveals *Ikbkap* deletion causes apoptosis of $Pax3^+$ progenitors and peripheral neurons. *Proc Natl Acad Sci* **110:** 18698–18703.

Heinicke LA, Nabet B, Shen S, Jiang P, van Zalen S, Cieply B, Russell JE, Xing Y, Carstens RP. 2013. The RNA binding protein RBM38 (RNPC1) regulates splicing during late erythroid differentiation. *PLoS One* **8:** e78031.

Hims MM, Ibrahim EC, Leyne M, Mull J, Liu L, Lazaro C, Shetty RS, Gill S, Gusella JF, Reed R, et al. 2007a. Therapeutic potential and

mechanism of kinetin as a treatment for the human splicing disease familial dysautonomia. *J Mol Med (Berl)* **85:** 149–161.

Hims MM, Shetty RS, Pickel J, Mull J, Leyne M, Liu L, Gusella JF, Slaugenhaupt SA. 2007b. A humanized *IKBKAP* transgenic mouse models a tissue-specific human splicing defect. *Genomics* **90:** 389–396.

Hui J, Stangl K, Lane WS, Bindereif A. 2003. HnRNP L stimulates splicing of the eNOS gene by binding to variable-length CA repeats. *Nat Struct Biol* **10:** 33–37.

Ibrahim EC, Hims MM, Shomron N, Burge CB, Slaugenhaupt SA, Reed R. 2007. Weak definition of *IKBKAP* exon 20 leads to aberrant splicing in familial dysautonomia. *Hum Mutat* **28:** 41–53.

Kastner B, Lührmann R. 1989. Electron microscopy of U1 small nuclear ribonucleoprotein particles: shape of the particle and position of the 5′ RNA terminus. *EMBO J* **8:** 277–286.

Kataoka N, Yong J, Kim VN, Velazquez F, Perkinson RA, Wang F, Dreyfuss G. 2000. Pre-mRNA splicing imprints mRNA in the nucleus with a novel RNA-binding protein that persists in the cytoplasm. *Mol Cell* **6:** 673–682.

Keren H, Donyo M, Zeevi D, Maayan C, Pupko T, Ast G. 2010. Phosphatidylserine increases IKBKAP levels in familial dysautonomia cells. *PLoS One* **5:** e15884.

Krainer AR, Maniatis T. 1985. Multiple factors including the small nuclear ribonucleoproteins U1 and U2 are necessary for pre-mRNA splicing in vitro. *Cell* **42:** 725–736.

Krainer AR, Conway GC, Kozak D. 1990. Purification and characterization of pre-mRNA splicing factor SF2 from HeLa cells. *Genes Dev* **4:** 1158–1171.

Kuroyanagi H, Ohno G, Mitani S, Hagiwara M. 2007. The Fox-1 family and SUP-12 coordinately regulate tissue-specific alternative splicing in vivo. *Mol Cell Biol* **27:** 8612–8621.

Kuroyanagi H, Ohno G, Sakane H, Maruoka H, Hagiwara M. 2010. Visualization and genetic analysis of alternative splicing regulation in vivo using fluorescence reporters in transgenic *Caenorhabditis elegans*. *Nat Protoc* **5:** 1495–1517.

Kuwasako K, Takahashi M, Unzai S, Tsuda K, Yoshikawa S, He F, Kobayashi N, Guntert P, Shirouzu M, Ito T, et al. 2014. RBFOX and SUP-12 sandwich a G base to cooperatively regulate tissue-specific splicing. *Nat Struct Mol Biol* **21:** 778–786.

Le MT, Xie H, Zhou B, Chia PH, Rizk P, Um M, Udolph G, Yang H, Lim B, Lodish HF. 2009. MicroRNA-125b promotes neuronal differentiation in human cells by repressing multiple targets. *Mol Cell Biol* **29:** 5290–5305.

Lee G, Papapetrou EP, Kim H, Chambers SM, Tomishima MJ, Fasano CA, Ganat YM, Menon J, Shimizu F, Viale A, et al. 2009. Modelling pathogenesis and treatment of familial dysautonomia using patient-specific iPSCs. *Nature* **461:** 402–406.

Lee G, Ramirez CN, Kim H, Zeltner N, Liu B, Radu C, Bhinder B, Kim YJ, Choi IY, Mukherjee-Clavin B, et al. 2012. Large-scale screening using familial dysautonomia induced pluripotent stem cells identifies compounds that rescue *IKBKAP* expression. *Nat Biotechnol* **30:** 1244–1248.

Lim KH, Ferraris L, Filloux ME, Raphael BJ, Fairbrother WG. 2011. Using positional distribution to identify splicing elements and predict pre-mRNA processing defects in human genes. *Proc Natl Acad Sci* **108:** 11093–11098.

Liu B, Anderson SL, Qiu J, Rubin BY. 2013. Cardiac glycosides correct aberrant splicing of *IKBKAP*-encoded mRNA in familial dysautonomia derived cells by suppressing expression of SRSF3. *FEBS J* **280:** 3632–3646.

Lundquist EA, Herman RK, Rogalski TM, Mullen GP, Moerman DG, Shaw JE. 1996. The mec-8 gene of *C. elegans* encodes a protein with two RNA recognition motifs and regulates alternative splicing of unc-52 transcripts. *Development* **122:** 1601–1610.

Mayeda A, Krainer AR. 1992. Regulation of alternative pre-mRNA splicing by hnRNP A1 and splicing factor SF2. *Cell* **68:** 365–375.

Miyamoto S, Hidaka K, Jin D, Morisaki T. 2009. RNA-binding proteins Rbm38 and Rbm24 regulate myogenic differentiation via p21-dependent and -independent regulatory pathways. *Genes Cells* **14:** 1241–1252.

Morini E, Dietrich P, Salani M, Downs HM, Wojtkiewicz GR, Alli S, Brenner A, Nilbratt M, LeClair JW, Oaklander AL, et al. 2016. Sensory and autonomic deficits in a new humanized mouse model of familial dysautonomia. *Hum Mol Genet* **25:** 1116–1128.

Ohe K, Mayeda A. 2010. HMGA1a trapping of U1 snRNP at an authentic 5′ splice site induces aberrant exon skipping in sporadic Alzheimer's disease. *Mol Cell Biol* **30:** 2220–2228.

Ohno G, Ono K, Togo M, Watanabe Y, Ono S, Hagiwara M, Kuroyanagi H. 2012. Muscle-specific splicing factors ASD-2 and SUP-12 cooperatively switch alternative pre-mRNA processing patterns of the ADF/cofilin gene in *Caenorhabditis elegans*. *PLoS Genet* **8:** e1002991.

Patton JG, Porro EB, Galceran J, Tempst P, Nadal-Ginard B. 1993. Cloning and characterization of PSF, a novel pre-mRNA splicing factor. *Genes Dev* **7:** 393–406.

Rando TA, Blau HM. 1994. Primary mouse myoblast purification, characterization, and transplantation for cell-mediated gene therapy. *J Cell Biol* **125:** 1275–1287.

Riley CM, Day RL, Greeley DM, Langford W. 1949. Central autonomic dysfunction with defective lacrimation; report of five cases. *Pediatrics* **3:** 468–478.

Shu L, Yan W, Chen X. 2006. RNPC1, an RNA-binding protein and a target of the p53 family, is required for maintaining the stability of the basal and stress-induced p21 transcript. *Genes Dev* **20:** 2961–2972.

Siebel CW, Kanaar R, Rio DC. 1994. Regulation of tissue-specific P-element pre-mRNA splicing requires the RNA-binding protein PSI. *Genes Dev* **8:** 1713–1725.

Singh RK, Cooper TA. 2012. Pre-mRNA splicing in disease and therapeutics. *Trends Mol Med* **18:** 472–482.

Slaugenhaupt SA, Blumenfeld A, Gill SP, Leyne M, Mull J, Cuajungco MP, Liebert CB, Chadwick B, Idelson M, Reznik L, et al. 2001. Tissue-specific expression of a splicing mutation in the *IKBKAP* gene causes familial dysautonomia. *Am J Hum Genet* **68:** 598–605.

Spena S, Tenchini ML, Buratti E. 2006. Cryptic splice site usage in exon 7 of the human fibrinogen β-chain gene is regulated by a naturally silent SF2/ASF binding site within this exon. *RNA* **12:** 948–958.

Sterne-Weiler T, Howard J, Mort M, Cooper DN, Sanford JR. 2011. Loss of exon identity is a common mechanism of human inherited disease. *Genome Res* **21:** 1563–1571.

Takeuchi A, Hosokawa M, Nojima T, Hagiwara M. 2010. Splicing reporter mice revealed the evolutionally conserved switching mechanism of tissue-specific alternative exon selection. *PLoS One* **5:** e10946.

Tanihata J, Suzuki N, Miyagoe-Suzuki Y, Imaizumi K, Takeda S. 2008. Downstream utrophin enhancer is required for expression of utrophin in skeletal muscle. *J Gene Med* **10:** 702–713.

Vacchi-Suzzi C, Hahne F, Scheubel P, Marcellin M, Dubost V, Westphal M, Boeglen C, Büchmann-Møller S, Cheung MS, Cordier A, et al. 2013. Heart structure-specific transcriptomic atlas reveals conserved microRNA-mRNA interactions. *PLoS One* **8:** e52442.

Warzecha CC, Sato TK, Nabet B, Hogenesch JB, Carstens RP. 2009. ESRP1 and ESRP2 are epithelial cell-type-specific regulators of FGFR2 splicing. *Mol Cell* **33:** 591–601.

Xu XQ, Soo SY, Sun W, Zweigerdt R. 2009. Global expression profile of highly enriched cardiomyocytes derived from human embryonic stem cells. *Stem Cells* **27:** 2163–2174.

Yang J, Hung LH, Licht T, Kostin S, Looso M, Khrameeva E, Bindereif A, Schneider A, Braun T. 2014. RBM24 is a major regulator of muscle-specific alternative splicing. *Dev Cell* **31:** 87–99.

Yoshida M, Kataoka N, Miyauchi K, Ohe K, Iida K, Yoshida S, Nojima T, Okuno Y, Onogi H, Usui T, et al. 2015. Rectifier of aberrant mRNA splicing recovers tRNA modification in familial dysautonomia. *Proc Natl Acad Sci* **112:** 2764–2769.

Zhou Z, Sim J, Griffith J, Reed R. 2002. Purification and electron microscopic visualization of functional human spliceosomes. *Proc Natl Acad Sci* **99:** 12203–12207.